

An ultrasonic feeding mechanism for continuous aerosol generation from cohesive powders

Lekhnath Pokharel¹, Prashant Parajuli¹, Li Li¹, Ewe Jiun Chng¹,
and Ranganathan Gopalakrishnan^{*1}

¹Department of Mechanical Engineering, The University of Memphis, Memphis, TN, USA

Supplemental Information (SI)

*Corresponding author: rgplkrsh@memphis.edu, Tel: 1-901-678-2580, Fax: 1-901-678-4180.

Information Available:

S1. Description of

(1) ultrasonic dispersion and de-agglomeration

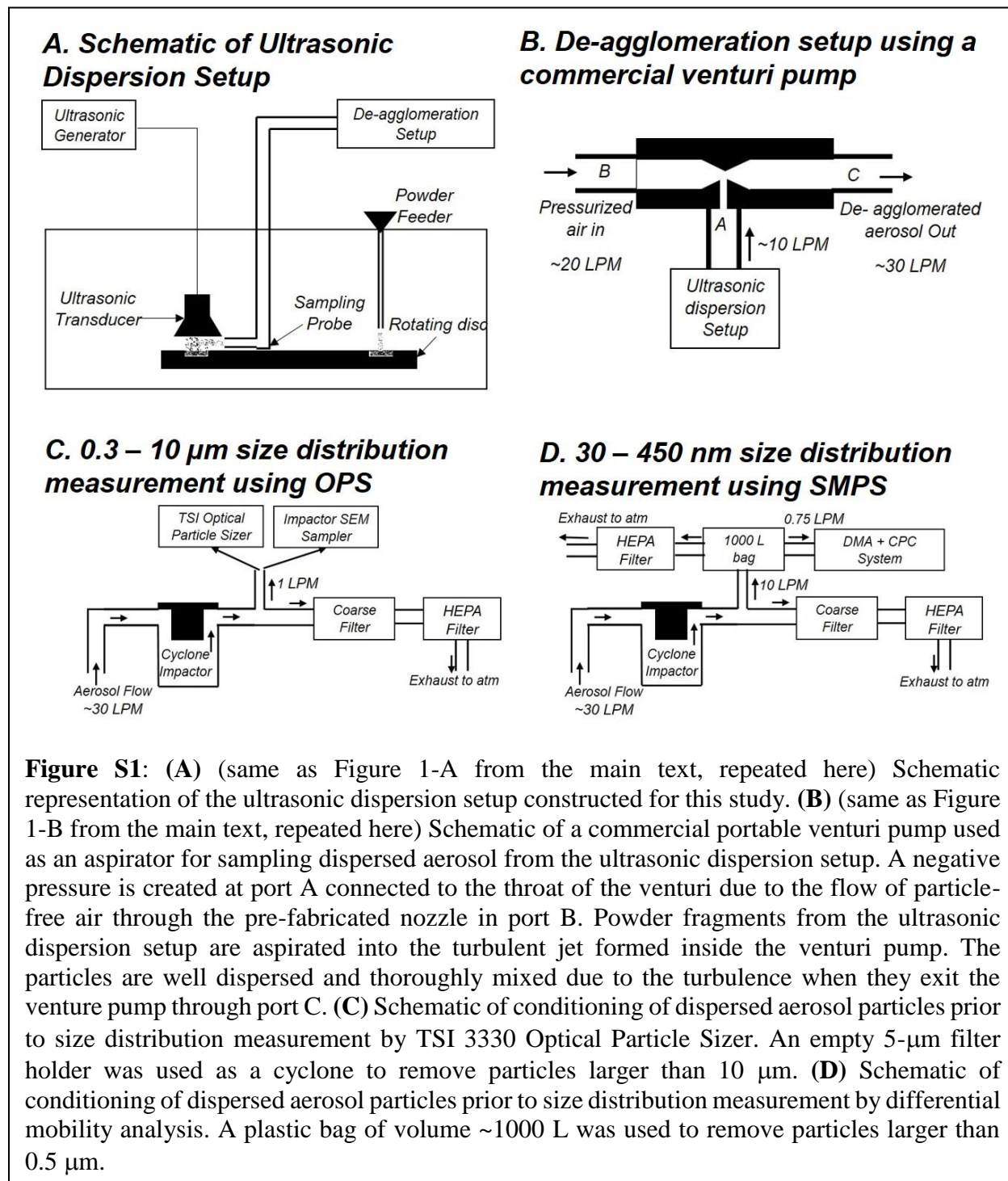
(2) size distribution measurement using TSI Optical Particle Sizer and Differential

Mobility Analysis

S2. SEM images and EDS data of particles imaged to characterization the aerosolization from powder phase

S3. Video of ultrasonic dispersion

S1. Description of 1) ultrasonic dispersion and de-agglomeration 2) size distribution measurement using TSI Optical Particle Sizer and Differential Mobility Analysis



0.3 – 10 μm aerosol size distribution measurement:

The aerosol exiting the venturi pump (volume flow rate ~ 30 LPM) is introduced into a cyclone for removing particles larger than $10\ \mu\text{m}$ prior to measurement (Fig. S1-C and S1-D). A standard $5\text{-}\mu\text{m}$ particulate filter holder (Central Pneumatic #68279) without a filter inside was used as a cyclone impactor. The size distribution downstream of the cyclone impactor was found to have particles no larger than $10\text{-}\mu\text{m}$ using a TSI 3330 Optical Particle Sizer (OPS). The OPS uses light scattering to detect particle size and to count individual particles in the $0.3\text{--}10\ \mu\text{m}$ size range and draws 1.0 LPM as sample flow. The instrument also circulates a 10 LPM sheath flow internally to improve the detection of particles by reducing aerosol beam broadening due to diffusion. After the OPS sampling, the bulk of the aerosol flow was exhausted to the atmosphere after filtration using a combination of coarse and HEPA filters (Fig. S1-C). The size distribution function calculated by the Aerosol Instrument Manager (AIM) software (TSI Inc.) is reported in this study.

Sub- $0.4\ \mu\text{m}$ aerosol size distribution measurement:

The size distribution of the particles in the sub- $0.4\ \mu\text{m}$ range was characterized using differential mobility analysis (Knutson and Whitby 1975). A 10 LPM portion of the aerosol flow was discharged into a homemade plastic bag (BARRICADE, #110CT60100LOWES6B, $6\ \text{mil}$) of volume ~ 1000 L to allow for the gas to expand to ambient conditions and for removing particles larger than $\sim 0.5\ \mu\text{m}$ by gravitational settling (Fig. S1-D). After ensuring steady-state concentration was established inside the 1000 L dispersion volume, aerosol particles were sampled for measurement (Fig. S1-D). A long column differential mobility analyzer, DMA (classification length= $44.444\ \text{cm}$, outer radius= $1.958\ \text{cm}$, inner radius= $0.937\ \text{cm}$) was used with a Kanomax FMT 3650 Condensation Particle Counter (CPC) to obtain the particle size distribution. A TSI 3088 soft X-ray bipolar charger was used to charge the particles to attain a known steady state charge distribution prior to detection (Fig. S3). The DMA was operated at a sheath flow of 7.5 LPM and the classification voltage was stepped (as opposed to commonly used exponential scanning(Wang and Flagan 1990)) in fixed increments between $50\ \text{V}$ – $10000\ \text{V}$ to cover the size range of $\sim 30\ \text{nm}$ – $450\ \text{nm}$. The sample flow exiting the DMA was maintained at 0.6 LPM to obtain a non-diffusing



Fig. S2: Pictures and hyperlinks for the two venturi pumps used – TD260LSS generates low-intensity vacuum while UV143H generates high intensity vacuum

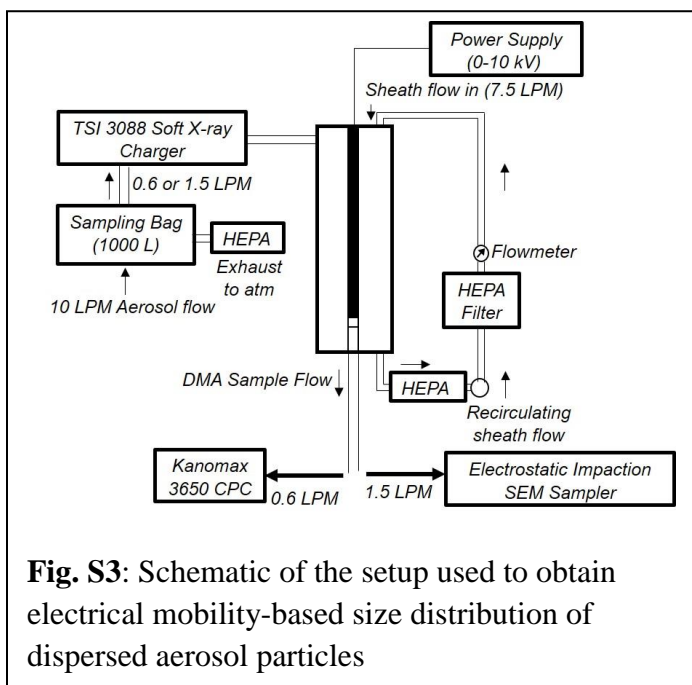


Fig. S3: Schematic of the setup used to obtain electrical mobility-based size distribution of dispersed aerosol particles

mobility resolution of ~ 12.5 . The digital pulses from the CPC were counted using the pulse counter on a National InstrumentTM USB 6002 data acquisition module using an in-house LabView[®] routine. All flowrates and voltages were calibrated to within $\pm 1\%$ accuracy using the Gilian[®] giliberator flow cell and high voltage probe (B&K Precision PR 28A) respectively. The recorded concentrations at each voltage was used to calculate the size distribution function using the Twomey-Markowski algorithm, described in detail in Buckley and Hogan Jr (2017), while accounting for multiple charging of particles (Gunn 1955, Wiedensohler 1988, Gopalakrishnan et al. 2013). From the SEM images, the particles were observed to have dense compact shapes and hence the reported mobility sizes can be considered representative, as the effect of shape of relatively compact shapes on the bipolar charging has been known to be small (Gopalakrishnan et al. 2013).

SEM Imaging of powder and dispersed phase particles: SEM images of the powders were obtained by smearing directly on a SEM stub with double-sided conducting adhesive carbon tape. To examine the aerosolized particles for each of the four powders studied, particles were collected from the gas phase on a SEM stub functioning as a single stage impactor in place of the OPS while drawing the same 1.0 LPM flow rate. For the 100 nm and 30 nm TiO₂ aerosol particles, to investigate the structure of particles in the sub-300 nm size range, mobility classified particles were collected downstream of the DMA. The same impactor was used with voltage applied (~ 1 kV) between the tip of the flow tube and the SEM stub (~ 1 cm spacing) to deposit all charged particles at a flow rate of 1.5 LPM. Since the size distributions of the sub-0.4 μm aerosol was broad, the voltage was continuously stepped for the sampling duration to collect all the particles that contribute to the observed size distribution through electrical mobility analysis. To confirm that the collected aerosol particles are made of TiO₂, Energy Dispersive X-ray Spectroscopy (EDS) was used to simultaneously obtain the atomistic composition of imaged particles.

S2. SEM images of particles imaged to characterization the aerosolization from powder phase

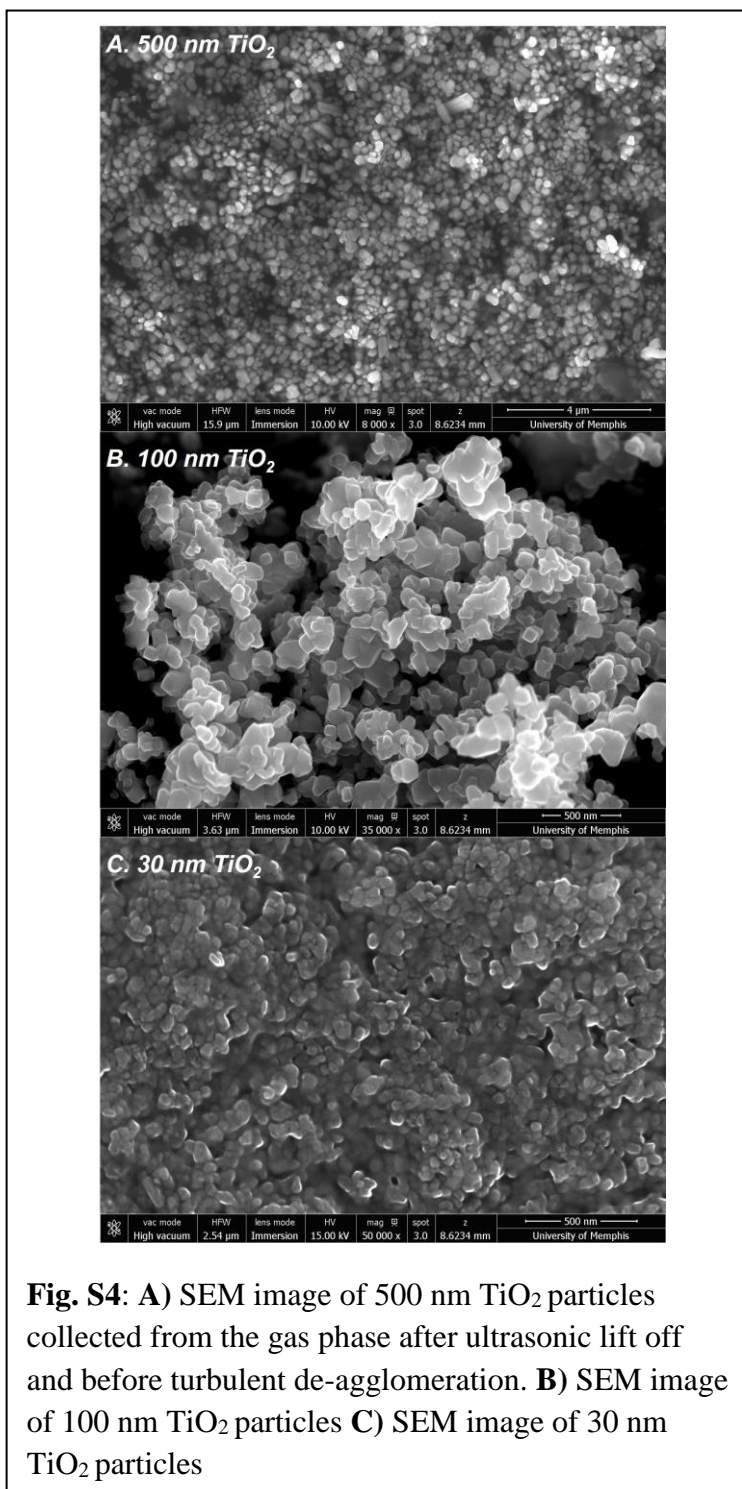


Fig. S5: 5 μm polyimide particles

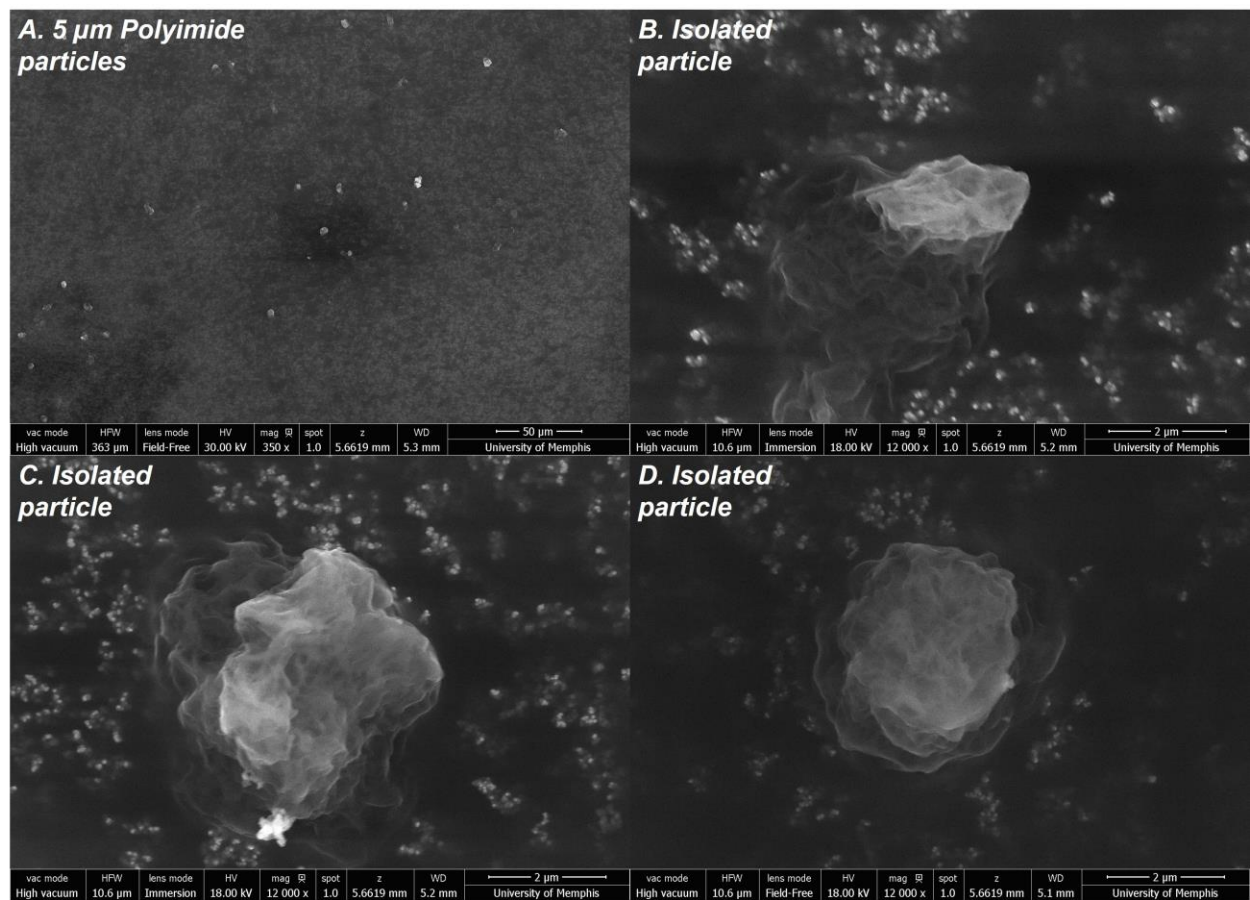


Fig. S6-1: 500 nm powder (SEM images)

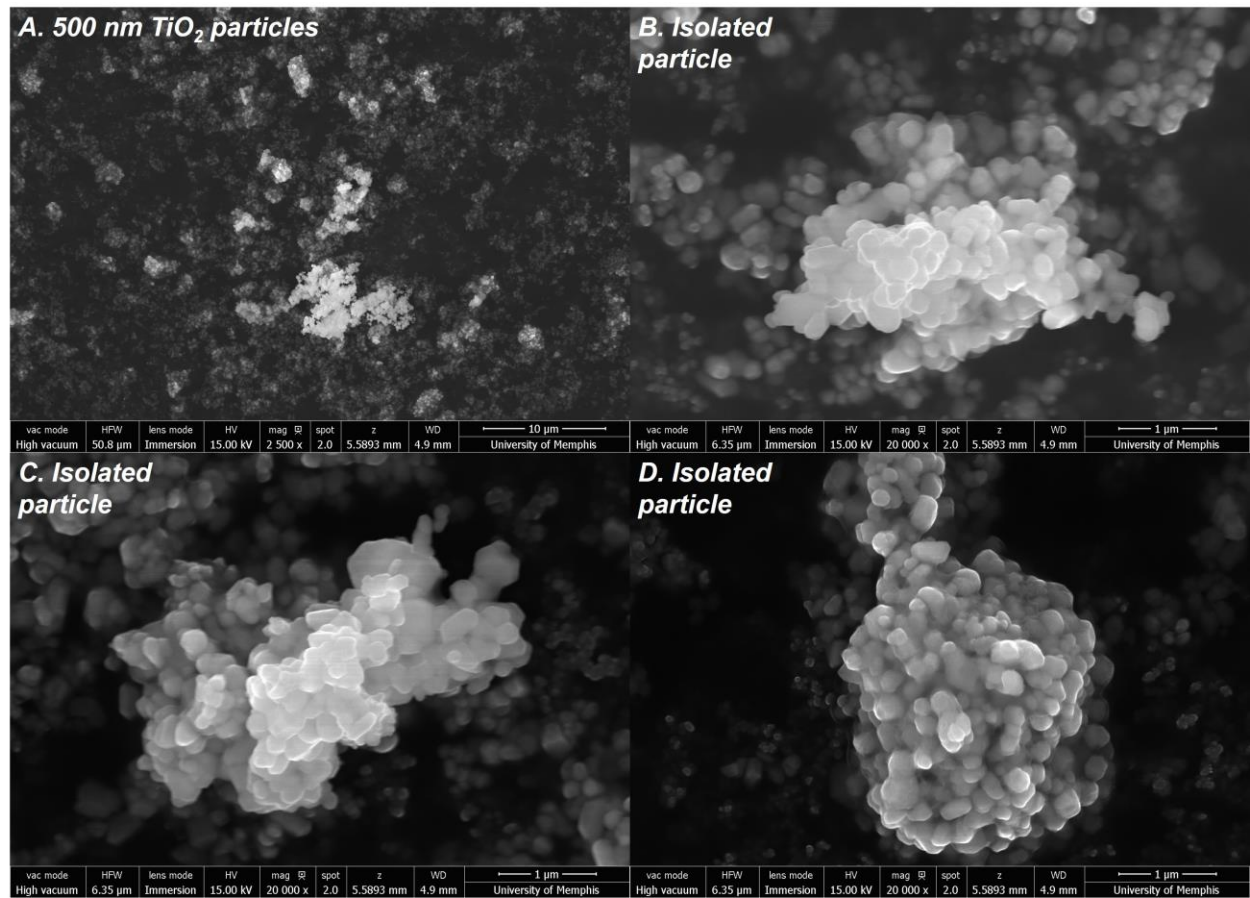


Fig. S6-2: 500 nm powder particle (EDS)

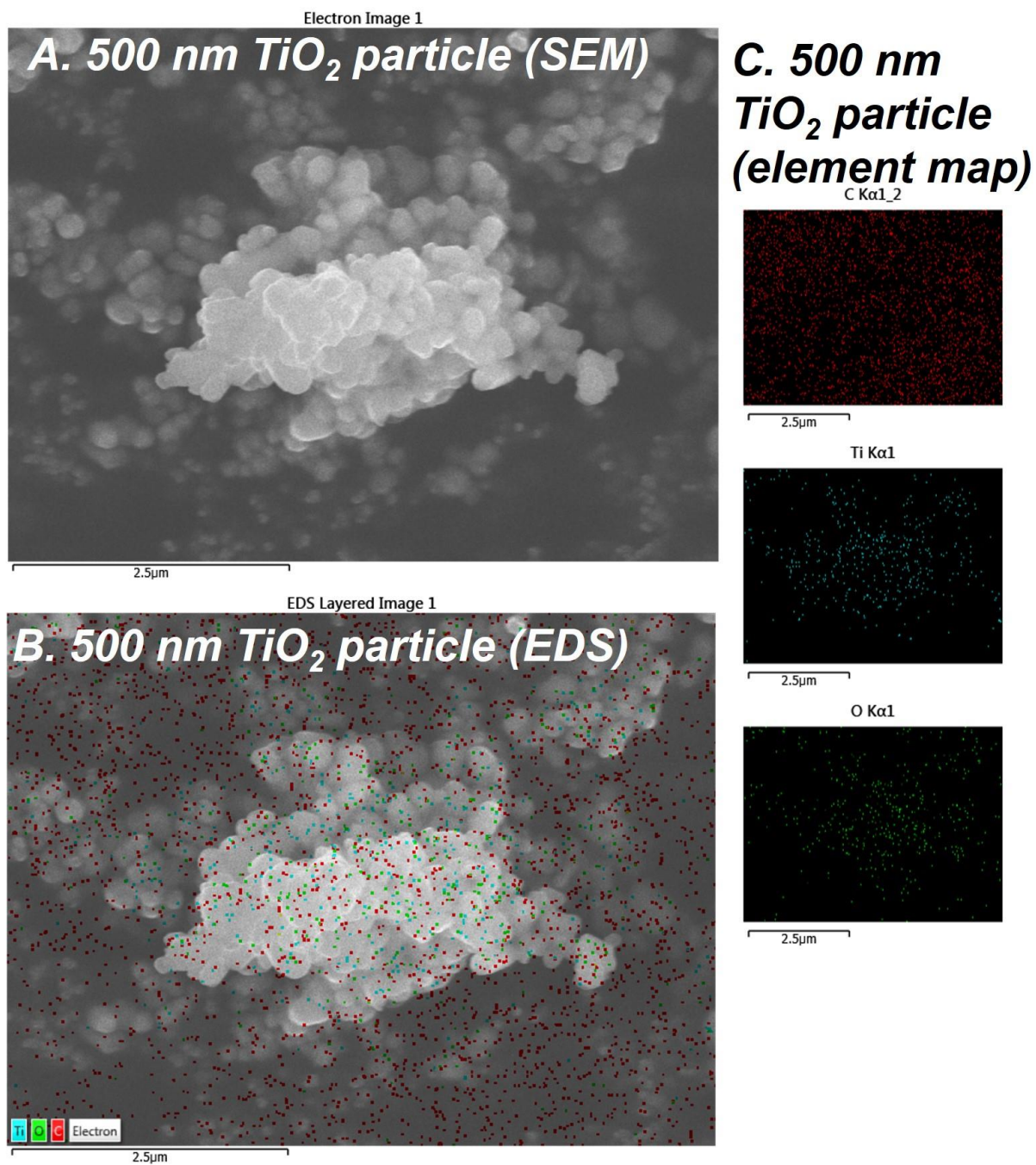


Fig. S6-3: 500 nm powder particle (EDS)

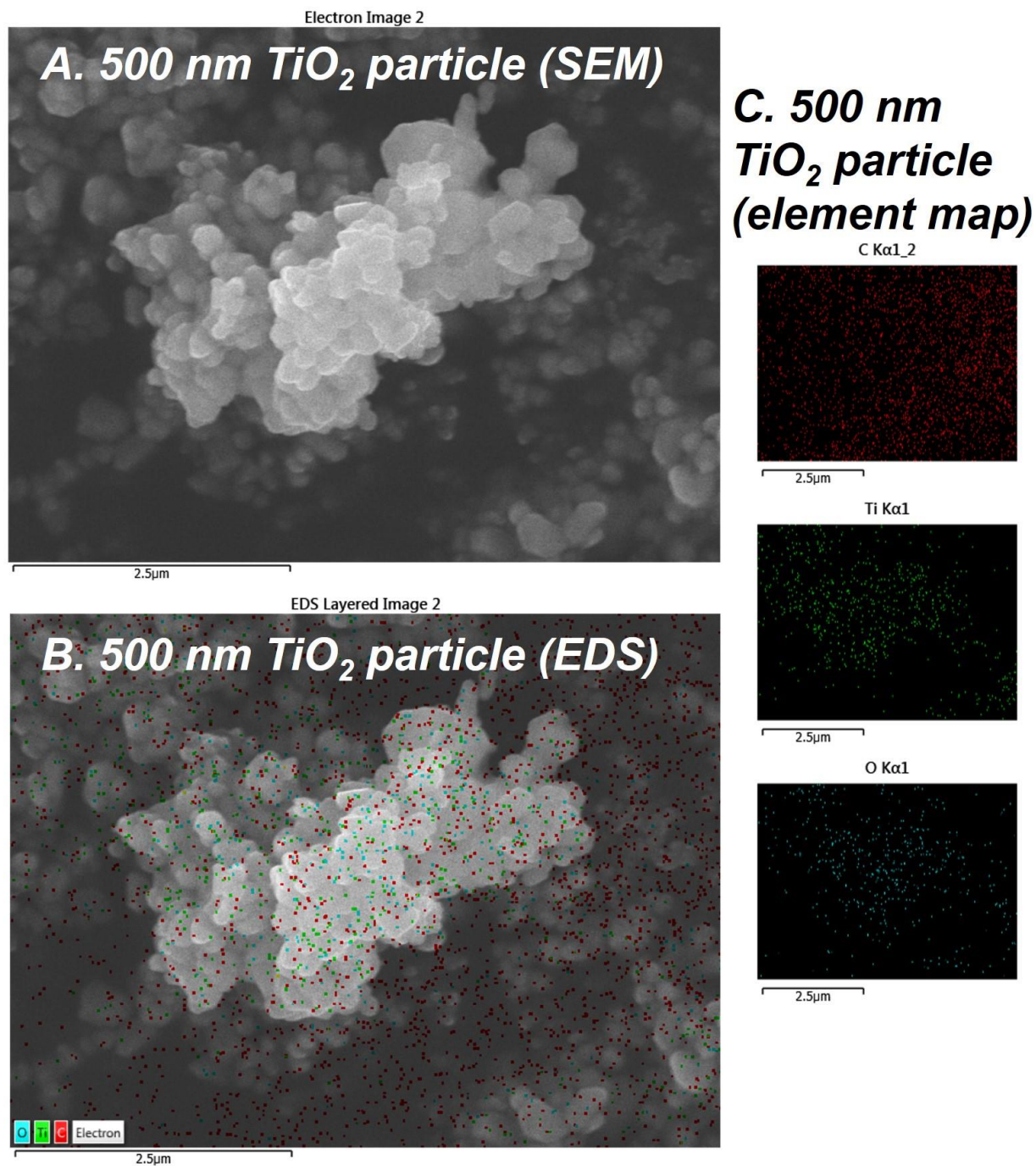


Fig. S7-1: 100 nm powder particles (SEM)

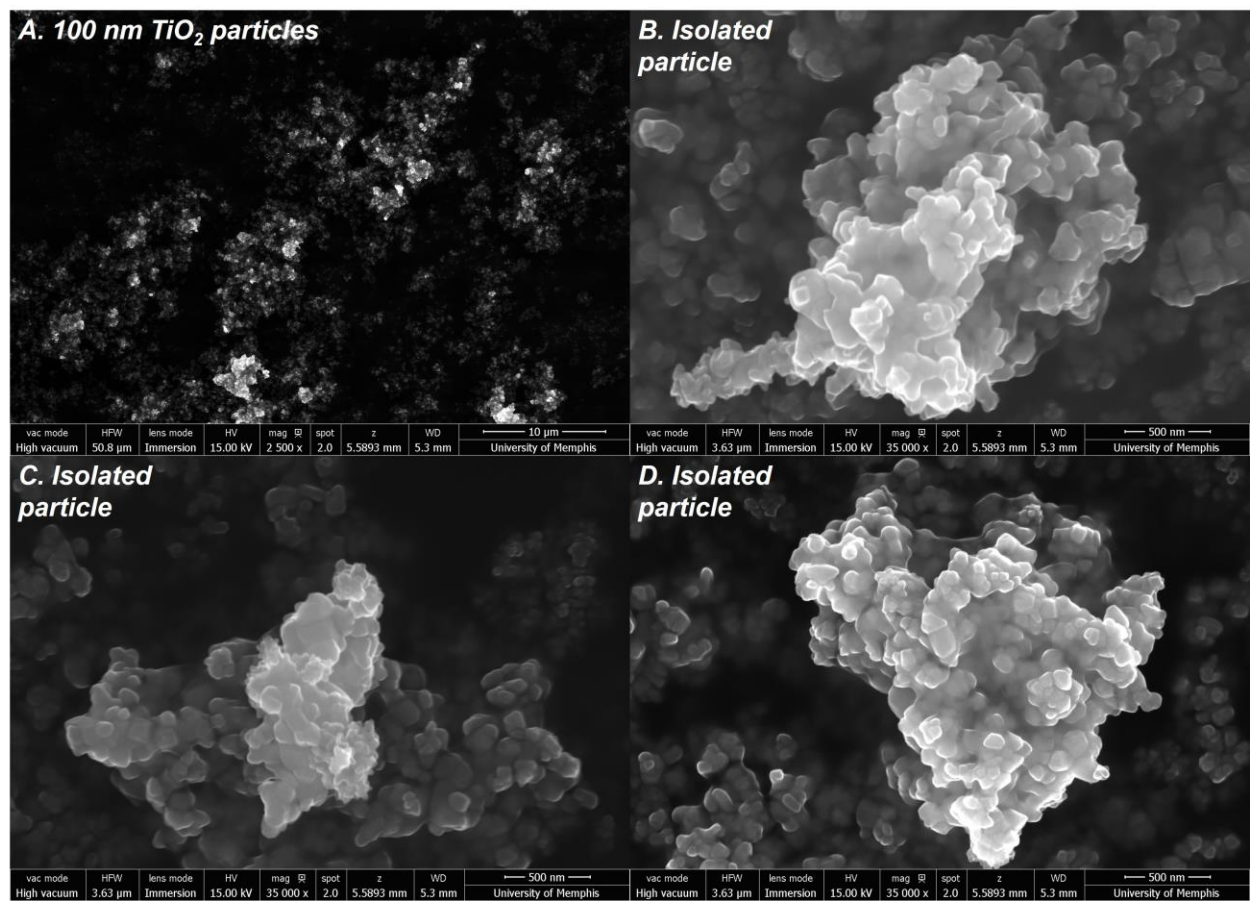


Fig. S7-2: 100 nm powder particles (EDS)

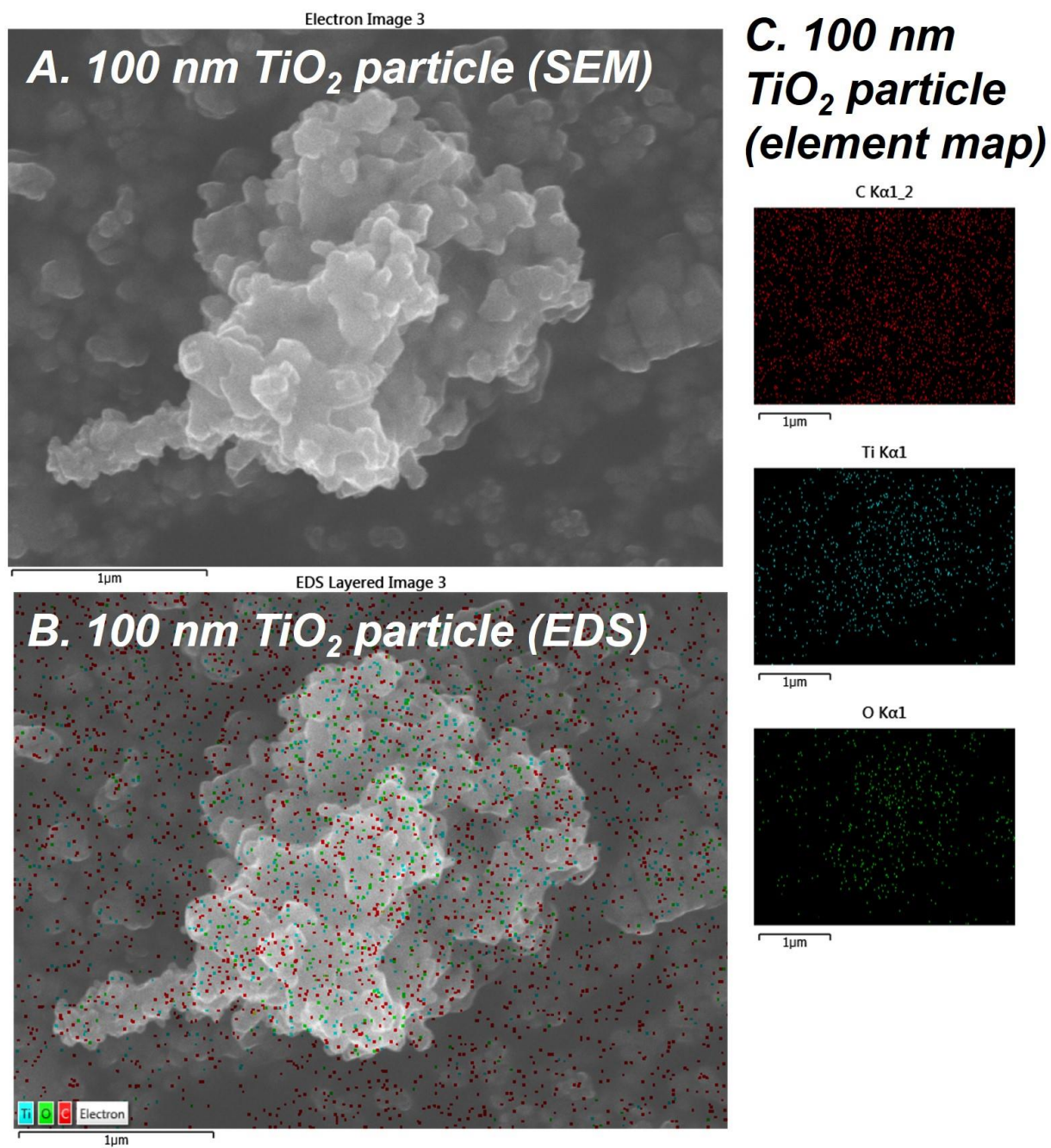


Fig. S7-3: 100 nm powder particles (EDS)

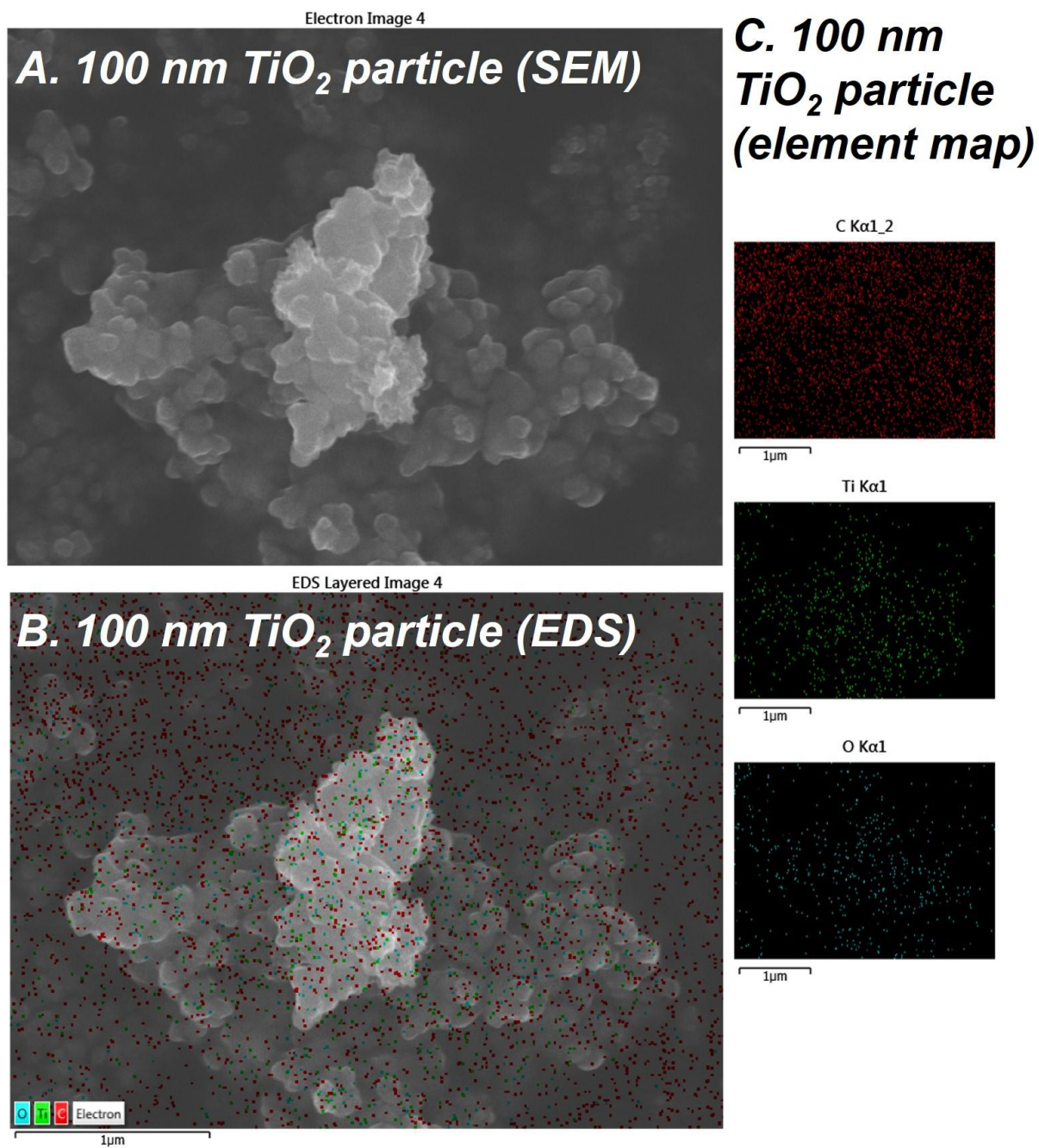


Fig. S8-1: 30 nm powder particles (SEM)

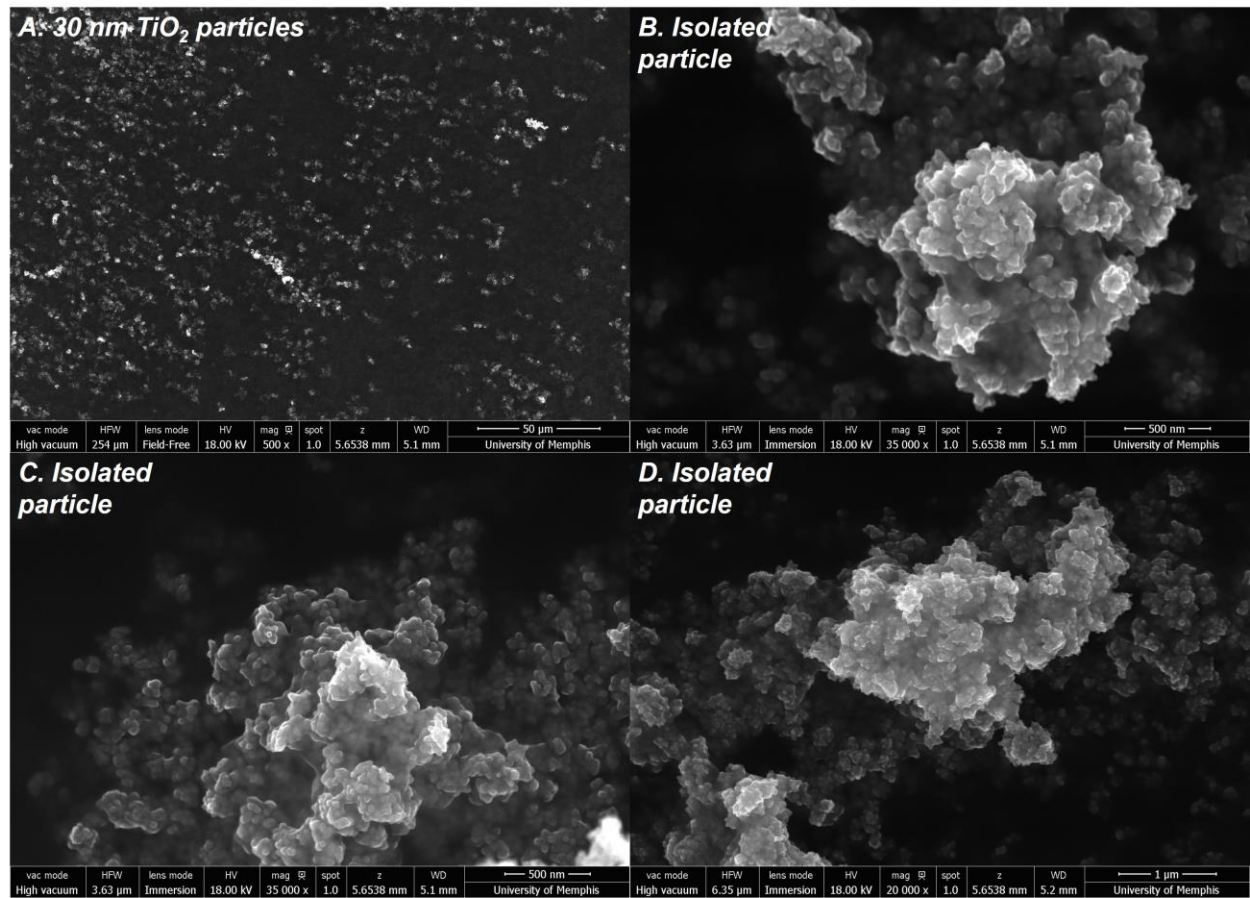


Fig. S8-2: 30 nm powder particles (EDS)

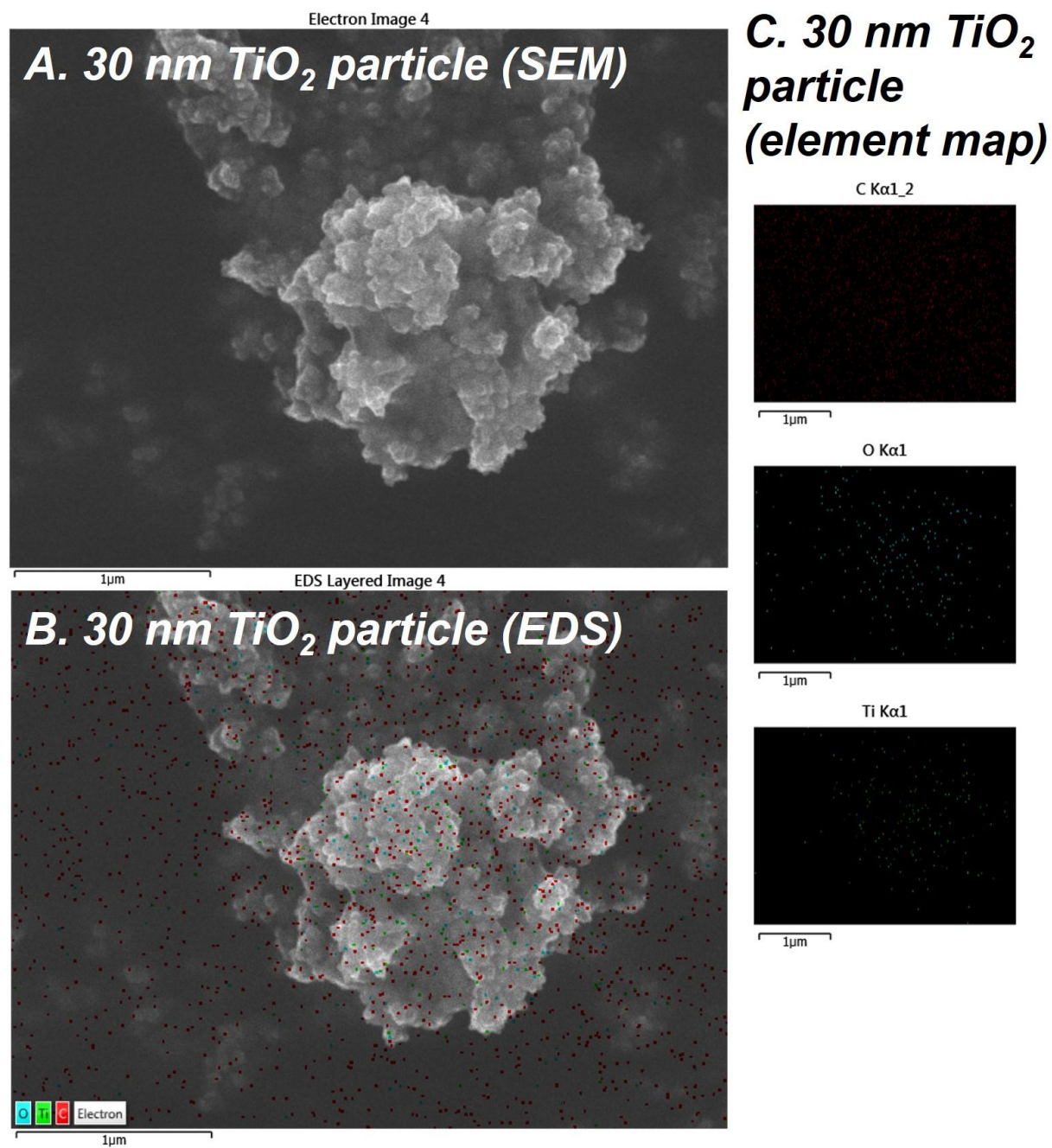
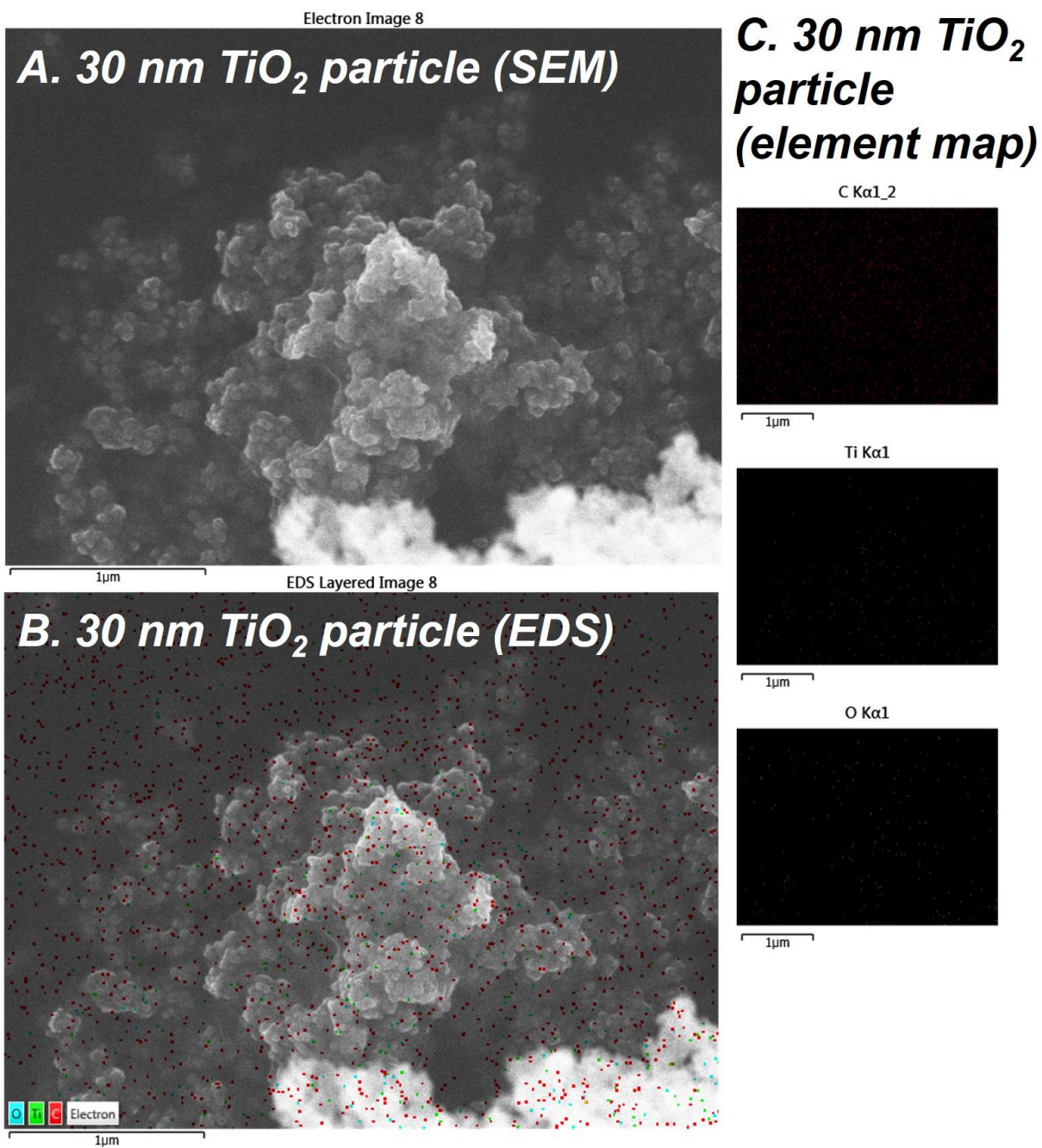


Fig. S8-3: 30 nm powder particles (EDS)



REFERENCES

1. Buckley, D. T. and C. J. Hogan Jr (2017). "Determination of the Transfer Function of an Atmospheric Pressure Drift Tube Ion Mobility Spectrometer for Nanoparticle Measurements." Analyst.
2. Gopalakrishnan, R., M. J. Meredith, C. Larriba-Andaluz and C. J. Hogan Jr (2013). "Brownian dynamics determination of the bipolar steady state charge distribution on spheres and non-spheres in the transition regime." Journal of Aerosol Science **63**(0): 126-145.
3. Gunn, R. (1955). "The statistical electrification of aerosols by ionic diffusion." Journal of Colloid Science **10**(1): 107-119.
4. Knutson, E. O. and K. T. Whitby (1975). "Aerosol classification by electric mobility: apparatus, theory, and applications." Journal of Aerosol Science **6**(6): 443-451.
5. Wang, S. C. and R. C. Flagan (1990). "Scanning Electrical Mobility Spectrometer." Aerosol Science and Technology **13**(2): 230-240.
6. Wiedensohler, A. (1988). "An Approximation of the Bipolar Charge-Distribution for Particles in the Sub-Micron Size Range." Journal of Aerosol Science **19**(3): 387-389.